GA–A27957

EXPANDING THE PHYSICS BASIS OF THE BASELINE Q=10 SCENRAIO TOWARD ITER CONDITIONS

by

T.C. LUCE, C. PAZ-SOLDAN, T.W. PETRIE, W.M. SOLOMON, F. TURCO, N. COMMAUX, A.M. GAROFALO, J.M. HANSON, G.L. JACKSON, R.I. PINSKER, and L. ZENG

SEPTEMBER 2014

GENERAL ATOMICS

DISCLAIMER

GA–A27957

EXPANDING THE PHYSICS BASIS OF THE BASELINE Q=10 SCENRAIO TOWARD ITER CONDITIONS

by
T.C. LUCE, C. PAZ-SOLDAN, T.W. PETRIE, W.M. SOLOMON,* F. TURCO,†
N. COMMAUX,‡ A.M. GAROFALO, J.M. HANSON,† G.L. JACKSON, R.I. PINSKER,
and L. ZENG¶

This is a preprint of a paper to be presented at the Twenty-Fifth IAEA Fusion Energy Conf., October 13-18, 2014 in Saint Petersburg, Russia, and to be published in the *Proceedings*.

*Princeton Plasma Physics Laboratory, Princeton, New Jersey.
†Columbia University, New York, New York.
‡Oak Ridge National Laboratory, Oak Ridge, Tennessee.
¶ University of California Los Angeles, Los Angeles, California.

Work supported by
the U.S. Department of Energy
under DE-FC02-04ER54698, DE-AC02-09CH11466, DE-FG02-04ER54761,
DE-AC05-00OR22725, and DE-FG02-08ER54984

GENERAL ATOMICS PROJECT 30200
SEPTEMBER 2014

GENERAL ATOMICS

Expanding the Physics Basis of the Baseline Q=10 Scenario Toward ITER Conditions

PPC/P2-34

T.C. Luce 1), C. Paz-Soldan 1), T.W. Petrie 1), W.M. Solomon 2), F. Turco 3), N. Commaux 4), A.M. Garofalo 1), J.M. Hanson 3), G.L. Jackson 1), R.I. Pinsker 1), and L. Zeng 5)

1) General Atomics, PO Box 85608, San Diego, CA, 93186-5608, USA.
2) Princeton Plasma Physics Laboratory, PO Box 4451, Princeton, NJ 08543-0451, USA.
3) Columbia University, New York, New York 10027, USA.
4) Oak Ridge National Laboratory, PO Box 3008, Oak Ridge, TN 37831, USA.
5) University of California Los Angeles, Los Angeles, CA 90095, USA.
e-mail contact of main author: luce@fusion.gat.com

Abstract. Key aspects of the ITER baseline scenario have been reproduced in DIII-D plasmas, with emphasis on areas where the ITER plasmas deviate significantly from most present-day experiments, namely, low core fueling, low torque input, and dominant electron heating. Normalized performance sufficient for the ITER objective is obtained. However, going from co- neutral beam injection (NBI) heating to balanced NBI or electron cyclotron heating leads to reduced confinement and additional challenges in plasma stability. Radiative solutions to aid the survivability of the divertor are demonstrated to be compatible with the ITER baseline scenario but have a clear cost in plasma performance. These results indicate that projections of ITER baseline scenario performance from the existing physics basis may be optimistic. A definitive understanding of these effects is needed, which will require experimental, theory, and modeling activity to both clarify the present situation and understand the expected implications for ITER.

1. Introduction

The first physics objective for the ITER project is to sustain a fusion power (P_{fus}) output of 500 MW for >300 s with an energy gain (Q) of 10. The baseline scenario to achieve this objective is an H-mode plasma of 15 MA at the nominal operating parameters (vacuum toroidal magnetic field B=5.3 T at major radius R=6.2 m with a single-null diverted cross-section with minor radius a=2.0 m). These conditions imply a normalized pressure [$\beta_N \equiv \langle p \rangle / (B^2/2\mu_0)/(I/aB)$] of 1.8% m T/MA and confinement quality H_{98y2}=1.0 are required to meet the objective with a safety factor near the edge (q_{95}) of 3. These metrics are considered reasonable from the existing tokamak physics basis [1,2]. The same conditions also imply that 50 MW of auxiliary heating power is required from the planned heating systems [neutral beam injection (NBI) at 1 MeV, electron cyclotron heating (ECH) at 170 GHz, and ion cyclotron heating (ICRH)] and sufficient flux is available from the solenoid.

While the existing physics basis supports the predicted performance of the baseline scenario including the extrapolation to smaller normalized gyroradius and collision frequency, there are significant qualitative differences between the plasmas in present-day tokamaks and those anticipated in ITER. The dominant contribution to the existing physics basis is from tokamaks with NBI heating with co-current injection geometry (co-NBI). This implies that there is a correlated central fueling and torque input with the heating power, which could modify the density and toroidal rotation profiles. These profiles affect impurity transport, energy transport, and stability. NBI heating in present tokamaks typically heats ions more than electrons, while both self-heating from the fusion α particles and all auxiliary heating systems for ITER heat predominantly the electrons. Further, ITER requires application of some technique for reducing both transient heat flux from the edge localized modes (ELMs) characteristic of H-mode operation and the steady-state heat flux to the divertor. These heat flux reductions are typically not applied to the plasmas for which the performance assessments were carried out. The DIII-D tokamak, because of the availability

of ECH, counter-current NBI, and the ability to reproduce the aspect ratio and poloidal cross-section of the ITER shape, is uniquely positioned to demonstrate how these differences from the bulk of the existing physics basis affect the performance projections.

Stationary plasmas in the ITER shape and matching the normalized performance parameters required of the ITER baseline have been made in DIII-D with low torque for up to ten resistive relaxation times (10 τ_R). Examples with dominant ion and electron heating are shown in Fig. 1. While these plasmas appear to be much alike despite the change in the heating method, there are important differences that are correlated with the change. These will be discussed more fully in the following sections as part of the more general discussion of the stability (Sec. 2) and transport (Sec. 3) in these ITER baseline plasmas. The effects of radiative divertor operation will be discussed in Sec. 4.

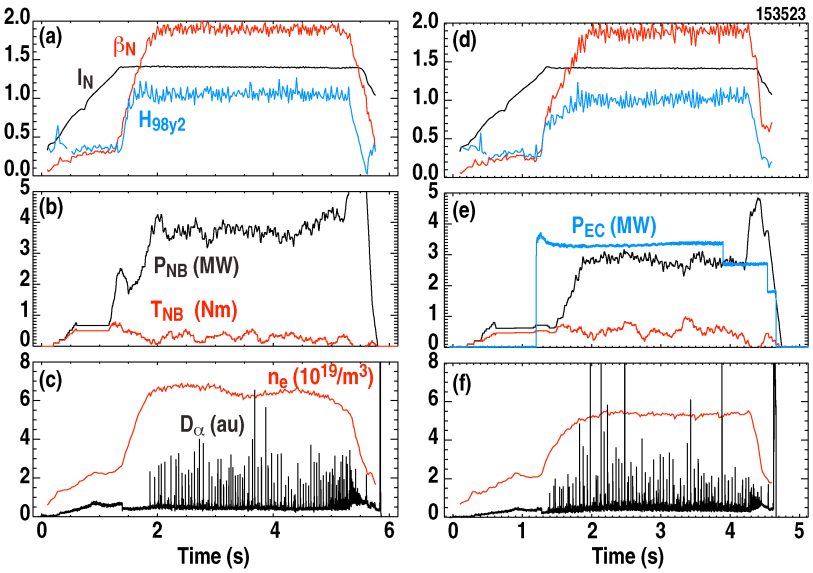

Fig. 1. Time histories of ITER baseline scenario plasmas with low applied torque and dominant ion heating (left column) or dominant electron heating (right column). Shown are (a,d) normalized pressure β_N (red), normalized current I(≡I/aB) (black), and confinement quality H_{98y2} (blue), (b,e) neutral beam power P_{NB} (MW) (black) neutral beam torque T_{NB} (N m) (red) and electron cyclotron heating power P_{EC} (MW) (blue), and (c,f) line-averaged density n (10^{19}/m^3) (red) and D_α light from the divertor (black).

2. Stability

The greatest obstacle to stationary operation in these ITER baseline scenario plasmas is the onset of an m=2/n=1 tearing mode. The onset condition for these modes is often discussed in terms of a pressure limit, but previous analysis has shown that this does not describe the mode onset in DIII-D plasmas with q_{95}=3 [3]. That analysis also showed that there is a lower bound on internal inductance for stable operation, but above this, it was possible to find both stable and unstable plasmas. Almost all of the plasmas discussed here have a current rise without auxiliary heating. Shortly after current flattop, the auxiliary heating is applied with the desired input torque, a transition to H mode occurs, and the pressure goes quickly to the desired operating level (Fig. 1). Initial work with low torque indicated that the stable operating space is reduced, when compared with the experience with co-NBI [4]. A database of >1100 DIII-D plasmas similar to the ITER baseline scenario has been compiled. Figure 2 illustrates that the plasmas with low applied torque (<1 Nm) terminate promptly (within 0.5τ_R of reaching the operating pressure) about 50% more frequently than the total population, consistent with the hypothesis that the operating space at low torque is more limited. The duration in Fig. 2 is defined as the time the operating pressure is maintained and is normalized to the current profile relaxation time. The median value of τ_R is 0.83 s. The normalization to τ_R is adopted because it should be the longest characteristic relaxation time in the plasma, but plotting versus absolute time or time normalized to energy confinement time yields similar plots. The duration in about 60% of all these plasmas, independent of the applied torque, is shorter than 2τ_R, a reasonable standard for the current profile in the outer part of the plasma to have come into equilibrium. This suggests that that there are actually two stability issues to address – determining whether there is a stationary operating point that is stable (t_{dur}/τ_R>2) and defining the limits on access

to this operating point ($t_{dur}/\tau_R<2$). Much of the experimental work in DIII-D to date has focused on establishing the existence of a stationary operating point; however, it is important to note that τ_R in ITER is ~200 s, indicating that defining the stable access conditions may be all that is required for ITER to meet its physics objective.

The hypothesis that the stability of the 2/1 tearing mode is set by the current profile is consistent with the majority of plasmas becoming unstable within a few τ_R (Fig. 2). However, between 10%-20% of the plasmas lasting more than $2\tau_R$ are still unstable to a 2/1 mode. Therefore, the database is a useful resource in testing hypotheses, but is unlikely to provide information on causality on its own. Issues that have been tested in experiments and will be discussed briefly include the role of uncorrected non-axisymmetric magnetic fields, the role of rotation, and the effect of ELMs. These issues are not independent from each other, so will be discussed together.

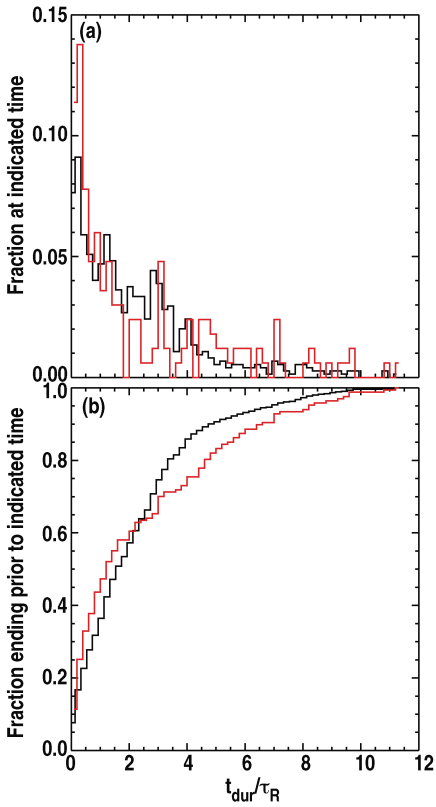

Fig. 2. Histograms of duration (t_{dur}) normalized to the current relaxation time (τ_R) for all ITER baseline plasmas (black) and low torque (red). The low torque plasmas comprise 22% of the total. (a) Fractional of occurrence at the specified time, (b) fractional occurrence prior to the specified time.

DIII-D has non-axisymmetric magnetic field structure due to various relative misalignments of the magnetic coils. The n=1 component is the most significant operationally and is routinely mitigated by an algorithm developed empirically. However, for these ITER baseline plasmas at low torque and low q_{95}, it was important to optimize the mitigation, since an uncorrected n=1 field might have the effect of inducing a 2/1 tearing mode. Optimal correction was based on minimization of the plasma response during the rise of β_N. A novel test to demonstrate that the correction was indeed optimized and determine the sensitivity to uncorrected n=1 fields was applied to the ITER baseline plasmas. This involved intentionally detuning the correction with an increasing amplitude and rotating phase about the optimum, and measuring both the plasma magnetic response and the toroidal rotation response to the detuning. Both responses are generally phase independent, indicating that the correction is indeed optimized. The rotation (or here angular momentum) response slowly grows (i.e., the plasma slows) until a critical value is reached when the plasma locks to the lab frame (Fig. 3). At lower rotation, the plasma is more sensitive to the magnetic perturbation, but sufficient correction can be applied. However, extrapolating linearly downward in momentum from the 1.05 Nm and 0.65 Nm cases to 0 Nm (assuming no nonlinear momentum degradation), Fig. 3 shows that, even with perfect correction, a plasma with no applied torque may be susceptible to the residual field that cannot be corrected with the existing coils. This point requires further investigation.

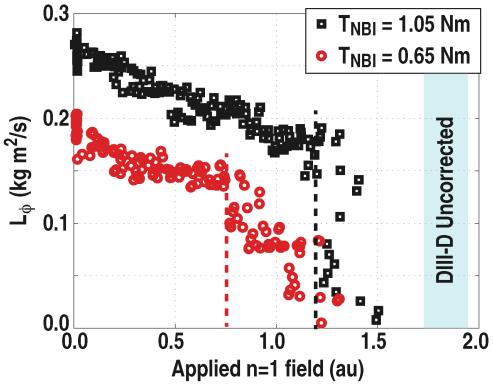

Fig. 3. Toroidal angular momentum L_ϕ (kg m^2/s) vs applied n=1 magnetic field (in units of equivalent coil current). The blue vertical bar indicates the range of the typical n=1 magnetic field in DIII-D without correction.

From the previous paragraph it is clear that it is difficult to determine whether rotation plays the role of cause or effect, since the penetration of a non-axisymmetric magnetic field into the plasma is screened by rotation, but also can apply resonant and non-resonant torques to the plasma. In addition, plasma transport may be affected by rotation through modification of the turbulence, which in turn will affect the current density profile through the parallel electrical conductivity. In order to try to separate these effects, step changes in rotation were applied to otherwise identical plasmas. In the absence of a step in the applied torque, the plasma rotation and internal inductance drop until an n=1 mode occurs at 2.8 s (black traces in Fig. 4). The cases with a 1 Nm increment in the applied torque from 2.3 s rotate faster and do not collapse (red and blue traces in Fig. 4). At 3.4 s, a negative increment of 1.5 Nm torque is applied to one of these plasmas (blue traces). When the toroidal rotation inside of the q=2 surface reaches approximately 2 kHz, this plasma becomes unstable (at the same value at which the plasma without the step became unstable). Together with the previous discussion on correcting the non-axisymmetric magnetic field, it appears that rotation plays an important role in the stability of these plasmas. It remains to be explained how it affects the stability and more importantly whether plasmas without rotation in the ITER baseline scenario can be stable.

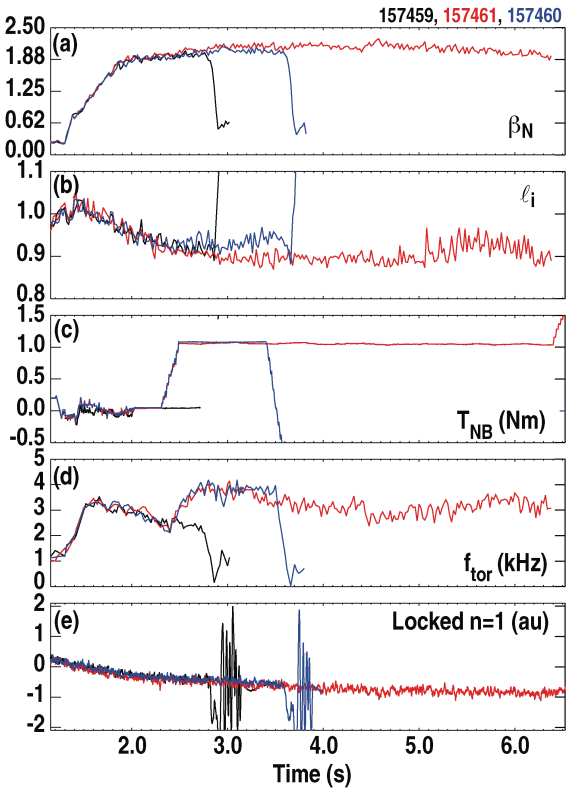

Fig. 4. Time histories of plasmas with variations in the applied torque – constant zero torque (black), 1 N m step up in torque (red), 1 N m step up in torque followed by a 1.5 N m step down in torque (blue). Shown are (a) normalized pressure β_N, (b) normalized internal inductance ℓ_i, (c) neutral beam torque (N m), (d) carbon rotation frequency just inside the q=2 surface f_{tor} (kHz), and (e) n=1 mode lock indicator.

Despite the clear correlation of stability with rotation, this is clearly not the entire story. Some baseline scenario plasmas have stationary rotation, yet evolve to an unstable state after many τ_R, as shown in the black traces of Fig. 5. In many cases, the ELM behavior becomes erratic, leading to upward excursions in the density accompanied by a secular upward trend, as shown here. In the process of probing the sensitivity of the plasma to uncorrected n=1 magnetic field by applying known n=1 perturbations, it was noted that the ELMs began to synchronize to the applied perturbations, leading to regular ELMs and stability to the n=1 tearing modes. With this knowledge, it was possible to use the magnetic perturbations as a pacemaker to maintain a regular ELM limit cycle and thereby maintain the stable conditions, as shown in the red traces in Fig. 5. Similar effects have been observed previously with n=3 fields [5]. The effect on the ELM period is shown in Fig. 6 where the time between ELMs is seen to be irregular without the n=1 perturbation but quite regular with it. The magnitude of the perturbation is equivalent to 0.5 on the x-axis of Fig. 3, so the effect on the rotation is relatively small. The mechanism by which the n=1 perturbation provokes the ELM is not clear, but it appears that square wave modulation is more effective than sine wave modulation for a given peak amplitude. The reason that the change in the ELM behavior affects the n=1 stability is also unclear; however, the fact that the internal inductance drops may indicate that the density increase in the pedestal increases the bootstrap current there, altering the balance

of the current density profile between the bootstrap-dominated pedestal and the inductively-driven core current with an adverse effect on the 2/1 stability.

The stability picture of the ITER baseline scenario with ITER-relevant values of applied torque appears to be quite complex, with imporant contributions from the current density, rotation, and density profiles which in turn are affected by the heating systems and non-axisymmetric fields. While this presents a rich and interesting platform for physics studies, it sounds a cautionary note on the robustness of this scenario for achieving the first physics objective for ITER.

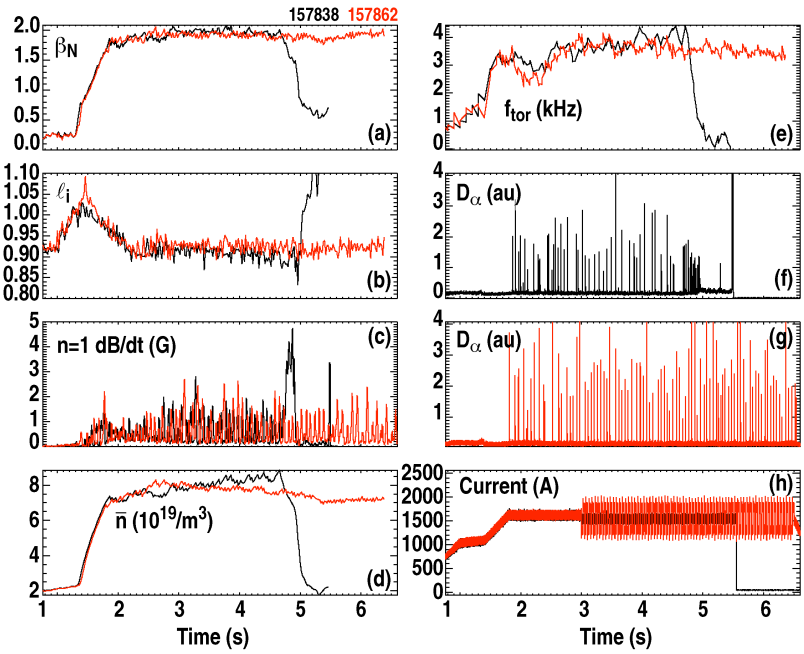

Fig. 5. Time histories of plasmas without (black) and with (red) ELM pacing with an applied n=1 magnetic field with square-wave amplitude modulation. (a) Normalized pressure β_N, (b) normalized internal inductance ℓ_i, (c) dB/dt from n=1 magnetic perturbations (G), (d) line-averaged density n (10^{19}/m^3), (e) carbon toroidal rotation just inside q=2 f_{tor} (kHz), (f) divertor D_α without ELM pacing, (g) divertor D_α with ELM pacing, (h) applied correction and pacing current in a single internal coil (A).

3. Confinement and Transport

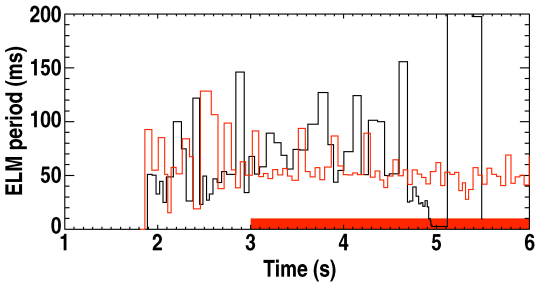

Fig. 6. Period between ELMs (ms) vs time (s) without (black) and with (red) ELM pacing. The red bar indicates the time period in which pacing fields are applied.

The standard metric for assessing the global confinement in H-mode plasmas is the IPB98y2 scaling [1]. As stated above, the majority of plasmas in the database from which this scaling was developed have dominant ion heating and co-current torque due to co-NBI. Experiments replicating the ITER baseline scenario have been carried out in the DIII-D tokamak comparing co-NBI plasmas to those with low applied torque due to more balanced NBI and with dominant electron heating due to ECH. For global confinement, the larger effect appears to be due to torque rather than heating method as shown in Fig. 7. The confinement quality, as measured by the ratio of the thermal confinement time to the IPB98y2 scaling (H_{98y2}) falls by 20% when comparing co-NBI to cases with low torque. By this measure, adding ~3 MW of ECH to similar plasmas yields the same values of H_{98y2}, when comparing cases with the same applied torque.

However, looking at individual plasmas with similar conditions, a more complicated picture emerges. Using H_{98y2} as the metric of confinement hides a substantial change in the global thermal confinement (τ_{th}) when ECH is applied to co-NBI plasmas [Fig. 8(a)]. The ECH deposition is near the half radius, but the sawtooth mixing radius is also near the half radius, so the off-axis deposition should not be the dominant cause of the factor of 2 drop in τ_{th}. Several factors that are expected to adversely affect confinement appear in the ECH case — the ratio of the ion to electron temperature drops, the rotation and rotational shear

drop, and Z_{eff} drops from 3 to 2. The latter is correlated with a qualitative change in the ELM behavior and reduced ion and electron temperature pedestal height in the ECH case. These effects are also likely connected with the drop in electron density [Fig. 8(b)] seen in the ECH case. The modest drop in H_{98y2}, even with a factor of 2 change in τ_{th}, is consistent with the strong power degradation in this scaling. The density dependence of the scaling also works to reduce the change in H_{98y2} in this case.

For the NBI only cases, the torque reduction also leads to a substantial reduction in τ_{th} [Fig. 8(a)], although not as large as seen with the application of ECH. The ratio of ion to electron temperature and Z_{eff} do not vary much across this scan, pointing to the rotation change as likely to play a significant role. The further addition of ECH reduces the density substantially [Fig. 8(b)], as well as Z_{eff}, but the confinement reduction is modest compared with the co-NBI case. This again points to the rotation profile as the key parameter. A variation of the rotation profile with changes in the applied torque is expected, but the significant change with ECH, while frequently observed, would not seem consistent with the conventional assumption that the momentum diffusivity can be described as a multiple of the ion heat diffusivity. These experiments point to the need for comprehensive modeling of particle, momentum, and heat transport to project present-day results to ITER.

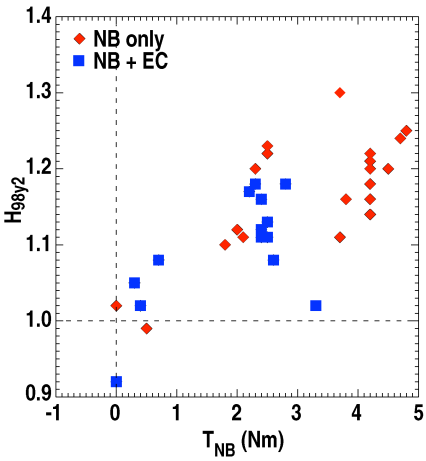

Fig. 7. Confinement quality H_{98y2} vs neutral beam torque T_{NB} (Nm).

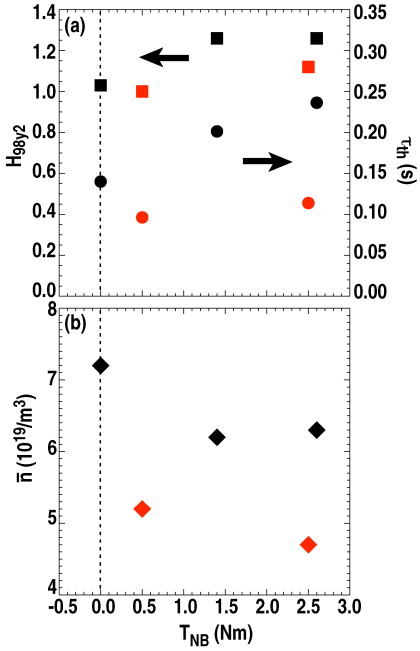

Fig. 8. (a) Confinement quality H_{98y2} (squares-left axis) and thermal confinement time τ_{th} (circles-right axis) vs neutral beam torque T_{NB} (Nm) for NBI only (black) and NBI+ECH (red). (b) line-averaged density n ($10^{19}/m^3$) vs neutral beam torque T_{NB} (Nm) for NBI only (black) and NBI+ECH (red).

4. Radiative Divertor Operation

Achieving the first physics objective in ITER implies 150 MW of loss power to the first wall must be handled. Most of this power is expected to flow into the scrape-off layer (SOL) and then into the divertor. As the width of the heat deposition in the SOL is anticipated to be quite narrow, some solution to dissipate the power spatially is required for the survivability of the divertor. In addition, the impulsive energy loads from ELMs are a major concern. One proposed solution to dissipating the heat is to use radiation in both the main chamber and the divertor to disperse the power more uniformly. It is important to consider both the efficacy of the heat dispersion and the impact on the core performance in assessing any solution to the heat flux problem. The experiments reported here explore the "puff and pump" radiative divertor scheme in plasmas like those described above that have the ITER shape and suitable normalized parameters to be consistent with the ITER baseline scenario. The heating from NBI was configured to be somewhat balanced but not down to levels that were ITER-relevant.

The first element in this scheme is to flow deuterium gas introduced in the main chamber down the SOL to the outer divertor leg, where there is an aperture for pumping (hence "puff and pump"). The gas puffing is necessary for both the radiation and improved retention of injected impurities (see below), but has a negative impact on the global energy confinement

(Fig. 9). The NBI is feedback controlled to maintain a constant stored energy of 0.9 MJ, so the increased power required reflects a reduction in confinement from about 0.19 s to 0.14 s. However, part of this reduction is due to the onset of an n=2 tearing mode [Fig. 9(c)]. From comparing the time histories of the power required, the effect of the 100 torr l/s flow (blue traces in Fig. 9) accounts for about half of the confinement reduction but the effects of the radiation and the tearing mode are neither linear nor additive.

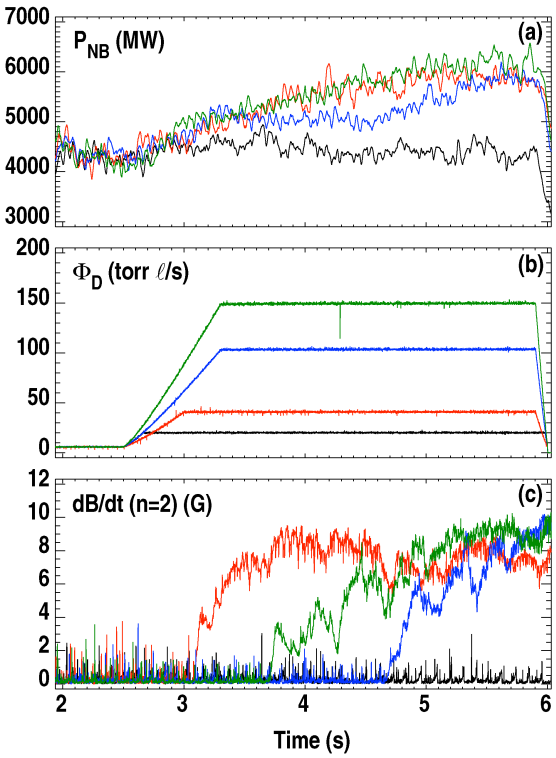

Fig. 9. Time histories of ITER baseline scenario plasmas with radiative divertor. (a) Neutral beam power P_{NB} (MW), (b) deuterium flow (torr l/s), (c) dB/dt from n=2 magnetic perturbations (G).

The benefits of the deuterium flow can be seen in the substantial reduction of the peak heat flux (Fig. 10). The peak heat flux at the outer divertor leg has been reduced in the time between ELMs and at an ELM by over 50%. This is consistent with the measured radiation shifting from the inner leg at low flow to the outer leg at high flow. At the highest flow rates, more than half of the input power is radiated outside of the plasma, indicating that the core confinement reduction is not due to excessive core radiation. The peak temperature on the outer divertor is reduced by 50%, but is actually increased for the inner divertor. The beneficial reduction of the peak heat flux during the ELM is due in part to an increase in the ELM frequency by more than a factor of 2.

The radiation effects can be further increased by introduction of an impurity gas in the private flux region. Here, neon was used. Again, the importance of the deuterium flow is seen by the reduction of neon found in the core plasma after puffing trace levels [Fig. 11(a)]. More than three times fewer neon ions are found in the core when substantial deuterium flows are present. With injection of sufficient neon to affect the radiation balance, the core concentration increased linearly up to the point where the plasma experienced a radiative collapse [Fig. 11(b)]. At the highest stable point, an additional 10% of the total power is radiated. Measurements of the radiation pattern indicate that much of this is coming from the pedestal region inside the plasma, complementing the radiation associated with the deuterium flow, which is primarily in the divertor region. There is a potential cost in terms of fusion production in that the contribution to Z_{eff} is 0.55 in this case. It will be important to pick the proper combination of impurity species, injection level, and deuterium flow to optimize the fusion output and divertor protection. The trade-offs can be illustrated in present-day experiments like these, but the choices for ITER will be sensitive to the actual plasma parameters since the radiation potential curves are very temperature sensitive.

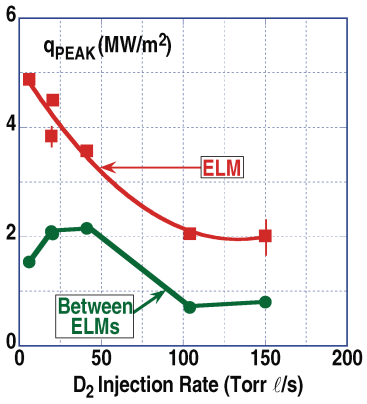

Fig. 10. Peak heat flux q_{PEAK} (MW/m^2) vs deuterium flow rate (torr l/s) between ELMs (green) and at an ELM (red).

5. Summary and Conclusions

Key aspects of the ITER baseline scenario have been reproduced in DIII-D plasmas, with emphasis on areas where the ITER plasmas should deviate significantly from the majority of present-day experiments. One area is the application of heating methods more similar to the heating expected in ITER both from fusion-produced α particles and the planned auxiliary heating systems. The relevant parameters here are low core fueling, low torque input, and dominant electron heating. In general, the trend from co-NBI heating to balanced NBI or ECH leads to reduced confinement and additional challenges in plasma stability. The source of the confinement reduction is not clearly identified, motivating future work in modeling and additional dedicated experiments to isolate the various effects. The physical mechanism behind the change in stability is also not clearly identified, due to a variety of phenomena leading to instability. However, in both cases, the rotation seems to play an important role, which motivates further theory and experimental work to understand momentum transport and sinks.

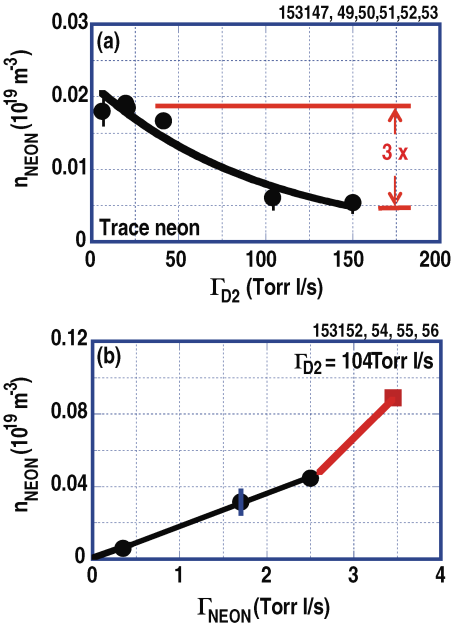

Fig. 11. (a) Core neon density n_{NEON} ($10^{19}/m^3$) for trace neon injection vs D_2 flow rate. (b) Core neon density n_{NEON} ($10^{19}/m^3$) vs neon flow rate for fixed D_2 flow of 10^4 torr l/s.

Radiative solutions to aid the survivability of the divertor are demonstrated to be compatible with the ITER baseline scenario but have a clear cost in plasma performance. The increased radiation comes with a reduction in the confinement and dilution of the plasma. However, the potential for radiation into the main chamber and in the divertor is substantial and may be necessary. Present estimates of the scaling of ELM loss energy to ITER indicate the mitigation seen here is likely not enough for the full performance ITER scenario, but the puff and pump radiative divertor may be important in the early phase of ITER to mitigate the ELMs while a comprehensive ELM stabilization scheme is established.

The principle conclusion from this work is that projections of ITER baseline scenario performance from the existing physics basis may be optimistic. All of the effects generally absent from the existing physics basis that were addressed with these experiments in DIII-D led to either performance reduction or scenario termination. This motivates two general research directions. First, an understanding of the effects observed here is needed, which will require experimental, theory, and modeling activity to both clarify the present situation and understand the expected implications for ITER. Second, the potential loss of performance margin for ITER motivates further research in alternate scenarios that may be more robust to these effects or have larger margin to tolerate any reduction in performance.

This material is based upon work supported by the U.S. Department of Energy, Office of Science, Office of Fusion Energy Sciences, using the DIII-D National Fusion Facility, a DOE Office of Science user facility, under Awards DE-FC02-04ER54698, DE-AC02-09CH11466, DE-FG02-04ER54761, DE-AC05-00OR22725, and DE-FG02-08ER54984.

References

[1] ITER Physics Basis, Nucl. Fusion **39**, 2137 (1999)
[2] Progress in the ITER Physics Basis, Nucl. Fusion **47**, S1 (2007)
[3] F. Turco and T.C. Luce, Nucl. Fusion **50**, 095010 (2010)
[4] G.L. Jackson et al., submitted to Nucl. Fusion (2014); and http://www-naweb.iaea.org/napc/physics/FEC/FEC2012/papers/275_EXP208.pdf
[5] W.M. Solomon, et al., Nucl. Fusion **52**, 033007 (2012)